JVI Journals.ASM.org

Comprehensive Mutational Analysis Reveals p6^{Gag} Phosphorylation To Be Dispensable for HIV-1 Morphogenesis and Replication

Benjamin Radestock,[a] Ivonne Morales,[a]* Sheikh Abdul Rahman,[a] Sonja Radau,[b] Bärbel Glass,[a] René Peiman Zahedi,[b] Barbara Müller,[a] Hans-Georg Kräusslich[a]

Department of Infectious Diseases, Virology, University of Heidelberg, Heidelberg, Germany[a]; Leibniz-Institut für Analytische Wissenschaften, Dortmund, Germany[b]

The structural polyprotein Gag of human immunodeficiency virus type 1 (HIV-1) is necessary and sufficient for formation of virus-like particles. Its C-terminal p6 domain harbors short peptide motifs that facilitate virus release from the plasma membrane and mediate incorporation of the viral Vpr protein. p6 has been shown to be the major viral phosphoprotein in HIV-1-infected cells and virions, but the sites and functional relevance of p6 phosphorylation are not clear. Here, we identified phosphorylation of several serine and threonine residues in p6 in purified virus preparations using mass spectrometry. Mutation of individual candidate phosphoacceptor residues had no detectable effect on virus assembly, release, and infectivity, however, suggesting that phosphorylation of single residues may not be functionally relevant. Therefore, a comprehensive mutational analysis was conducted changing all potentially phosphorylatable amino acids in p6, except for a threonine that is part of an essential peptide motif. To avoid confounding changes in the overlapping *pol* reading frame, mutagenesis was performed in a provirus with genetically uncoupled *gag* and *pol* reading frames. An HIV-1 derivative carrying 12 amino acid changes in its p6 region, abolishing all but one potential phosphoacceptor site, showed no impairment of Gag assembly and virus release and displayed only very subtle deficiencies in viral infectivity in T-cell lines and primary lymphocytes. All mutations were stable over 2 weeks of culture in primary cells. Based on these findings, we conclude that phosphorylation of p6 is dispensable for HIV-1 assembly, release, and infectivity in tissue culture.

The final steps in human immunodeficiency virus type 1 (HIV-1) replication are budding and release of viral particles from the host cell plasma membrane. The viral structural polyprotein Gag is sufficient for the production of virus-like particles *in vitro* (1) and in tissue culture (2) and is essential for virus particle formation in infected cells. Gag traffics to the plasma membrane, where it assembles into a curved lattice and recruits other viral proteins and genomic RNA. The assembly process culminates in budding of immature enveloped virions from the plasma membrane carrying a semispherical Gag shell (3–5). Concomitant with budding, the viral protease (PR) cleaves Gag into its mature subunits, matrix (MA), capsid (CA), nucleocapsid (NC), and p6, as well as two spacer peptides, SP1 and SP2, leading to maturation of the infectious virion (6).

In the mature particle, MA lines the viral envelope and CA forms the conical capsid shell surrounding the nucleoprotein complex, in which NC condenses the viral RNA genome (6). The C-terminal domain of HIV-1 Gag, p6, comprises the "late domains" of the virus, small peptide motifs that interact with components of the host cell endosomal complex required for transport (ESCRT) (reviewed in references 6, 7 and 8). Recruitment of a subset of the ESCRT machinery to the viral budding site mediates membrane constriction and the abscission of the virus from the host cell membrane. Late domains have been identified in Gag proteins of retroviruses and in structural proteins of several other enveloped viruses (9, 10). In the case of HIV-1, a P(T/S)AP motif and an LYPX$_n$LXXL motif interact with the ESCRT-I component TSG101 and the ESCRT-associated protein ALIX, respectively. In most cell lines, the P(T/S)AP motif is functionally dominant. Deletion or mutation of this motif results in the accumulation of late viral budding structures at the plasma membrane, connected by a thin membrane tether to the host cell (11). Structural analyses of HIV-1 budding sites and immature virus particles (4) and live-cell imaging of ESCRT recruitment to HIV-1 budding sites (12, 13) have suggested temporal regulation to coordinate Gag assembly and the formation of ESCRT complexes during HIV-1 assembly and budding.

The p6 domain of HIV-1 comprises 52 amino acids; it is largely unstructured (14, 15) and lacks distinct features besides the highly conserved late domains and motifs required for incorporation of the viral accessory protein Vpr (14, 16). However, p6 has been shown to be posttranslationally modified by monoubiquitinylation (17) and phosphorylation (18), and p6 is the predominant viral phosphoprotein in HIV-1 particles. Both types of modification are well known to play regulatory roles, sometimes connected in a sequential manner (reviewed, e.g., in reference 19), allowing their interplay and cross talk (20). Late-domain-carrying proteins of other viruses, e.g., murine leukemia virus (21), Mason-Pfizer monkey virus (22), Marburg virus (23), and vesicular stomatitis virus (24), are also phosphorylated. Phosphorylation of HIV-1 p6 was found to occur at multiple sites and to involve serine, threonine, and tyrosine residues (18); the exact sites of phosphorylation have not been determined, however.

Received 14 August 2012 **Accepted** 18 October 2012

Published ahead of print 31 October 2012

Address correspondence to Hans-Georg Kräusslich, Hans-Georg.Kraeusslich@med.uni-heidelberg.de.

* Present address: Ivonne Morales, Program in Physical Biology, NICHD/NIH, Bethesda, Maryland, USA.

Supplemental material for this article may be found at http://dx.doi.org/10.1128/JVI.02162-12.

doi:10.1128/JVI.02162-12

Several studies focused on individual potentially phosphorylated p6 residues, but the functional role of HIV-1 p6 phosphorylation remains largely enigmatic. Residue T23 of p6 can be phosphorylated by Erk kinase, and mutation of this residue was reported to result in a late-domain-deficient phenotype, with viral buds arrested at the plasma membrane and reduced bulk particle release (25). More recently, Votteler and coworkers (26) reported that an S40F mutation in p6 resulted in aberrant HIV-1 core formation and reduced viral infectivity, while bulk release efficiency was unaffected. A mechanistic connection between phosphorylation at either of these sites and HIV-1 release has not been identified, however. Since 13 of the 52 amino acids of p6 are potentially phosphorylatable and phosphorylation at several sites has been detected (18), mutational approaches are particularly difficult in this case. Furthermore, many proteins carry redundant phosphorylation sites (27), and mutation of individual residues thus may not necessarily be conclusive. Finally, the p6 coding sequence overlaps the *pol* reading frame in the HIV-1 genome, limiting the options for changing p6 without generating potentially confounding changes in *pol*.

Here, we made use of an HIV-1 variant in which the *gag* and *pol* reading frames were uncoupled by mutagenesis in order to investigate the role of p6 phosphorylation in infectious HIV-1 particle formation in a comprehensive manner. Candidate individual residues, multiple residues, or all phosphorylatable residues except T8, which is part of the PTAP motif essential for p6 function, were changed to nonphosphorylatable amino acids. The resulting mutant viruses were characterized for Gag phosphorylation status, particle formation, and infectivity in different cell lines and primary cells. Unexpectedly, even mutation of almost all phosphorylatable residues had only minor effects on virus release and infectivity, indicating that phosphorylation of $p6^{Gag}$ is dispensable for HIV-1 replication.

MATERIALS AND METHODS

Tissue culture and PBMC isolation. HeLa TZM-bI (28), HeLa (29), and human embryonic kidney 293T (30) cells were grown in Dulbecco's modified Eagle's medium (Invitrogen). T cells (C8166 [31] and MT-4 [32]) were cultivated in RPMI 1640 (Invitrogen). All media were supplemented with 10% fetal bovine serum (FBS) (Biochrom), 100 units/ml penicillin, 100 μg/ml streptomycin (Pen/Strep; Biochrom), and 10 mM HEPES (Sigma-Aldrich). Peripheral blood mononuclear cells (PBMCs) were isolated from buffy coats of healthy blood donors by Ficoll density gradient centrifugation following a standard protocol. For each experiment, PBMCs obtained from three different donors were used. Before infection, 4×10^6 cells were stimulated by growth in RPMI supplemented with 10 μg/ml interleukin-2 (IL-2) (Biomol) and 2 μg/ml phytohemagglutinin (PHA) (Sigma) for 3 days.

Plasmids and transfections. Infectious proviral constructs were based on plasmid pNL4-3 (33). Derivatives of pNL4-3 carrying single point mutations were produced by PCR-based site-directed mutagenesis using primers 5′GCCCCACCAGAAGAGGCCTTCAGGTTTGGGGAAG3′ (S14A), 5′GGAAGAGACAACAATTCCCTCTCAGCCGCAGG3′ (T23I), 5′GAAGAGACAACAACTCCCGCTCAGAAGCAGGAGCCG3′ (S25A), and 5′GGCAGCGACCCCTCGTAACAATAAAGATAGGG3′ (S51stop).

The plasmid $pNL4\text{-}3_{unc}$, uncoupling the *gag* and *pol* open reading frames (ORFs) of HIV-1, was constructed according to a previous report (34). A silent unique MluI restriction site was introduced into pNL4-3 at nucleotide position 1356 with respect to the start of the *gag* reading frame. Subsequently, an ApaI-MluI fragment was replaced by a 345-bp synthetic DNA fragment (GeneArt AG, Regensburg, Germany). In this fragment, the original slippery site and the stem-loop structure of the Gag-Pol frameshift signal were destroyed by point mutations. In addition, a new functional frameshift signal was introduced upstream of the *gag* stop codon according to the method of Leiherer et al. (34). This mutagenesis procedure resulted in extension of the *gag* reading frame by 15 bp. Furthermore, a unique silent ClaI restriction site was introduced at nucleotide position 1225 with respect to the start of the *gag* reading frame. This resulted in construct $pNL4\text{-}3_{unc}$ wild type (wt) carrying three unique restriction sites (XmaI, ClaI, and MluI) spanning the p6 region (Fig. 1D). Synthetic gene fragments (GeneArt AG, Regensburg, Germany) carrying mutations in potentially phosphorylated residues of p6 (Fig. 1D) were then cloned into $pNL4\text{-}3_{unc}$ wt to generate $pNL4\text{-}3_{unc}$ Nterm (with exchange of the XmaI-ClaI fragment), $pNL4\text{-}3_{unc}$ Cterm (ClaI-MluI fragment), and $pNL4\text{-}3_{unc}$ FL (XmaI-MluI fragment). Detailed cloning protocols and sequences of synthetic DNA fragments are available upon request.

Plasmids expressing enhanced green fluorescent protein (EGFP)-labeled Gag for live-cell imaging were constructed based on pCHIV and $pCHIV^{eGFP}$ (35). $pCHIV_{unc}$ and $pCHIV_{unc}{}^{eGFP}$ were constructed by replacing a SwaI fragment in pCHIV or $pCHIV^{eGFP}$ with the corresponding SwaI fragment from $pNL4\text{-}3_{unc}$. To construct $pCHIV_{unc}$ FL and $pCHIV_{unc}{}^{eGFP}$ FL, an ApaI-AgeI fragment comprising the *gag* region of $pNL4\text{-}3_{unc}$ FL was inserted into $pCHIV_{unc}$ and $pCHIV_{unc}{}^{eGFP}$.

Virus production, p24 ELISA, and infectivity assays. 293T cells were seeded at a density of 5×10^5/well (6-well plates) or 1.5×10^6/well (10-cm dishes). On the following day, the cells were transfected with 2 μg (6-well plate) or 10 μg (10-cm dishes) of the respective plasmid by a standard $CaPO_4$ method. At 30 h posttransfection (p.t.), the supernatants were harvested and cleared by centrifugation at 720 × *g* and 4°C for 10 min or filtration through 0.45-μm-pore-size filters. Virus production was quantitated by an in-house enzyme-linked immunosorbent assay (ELISA) detecting the HIV-1 CA protein p24 (36). To analyze single-round infectivity, 10^4 HeLa TZM-bl indicator cells were incubated with serial 5-fold dilutions of supernatants. At 48 h p.i., luciferase activity in cell lysates was determined using the Steady-Glo Luciferase Assay System (Promega). Relative light units (RLU) were normalized to virus amounts as determined by p24 ELISA. The 50% tissue culture infective dose ($TCID_{50}$) on C8166 T cells was determined by endpoint titration. For this, 3×10^4 cells/well were seeded in 96-well plates and infected with serial 10-fold dilutions in 6-fold replicates as described by Reed and Muench (37).

For infection experiments, stimulated PBMCs from two different donors were mixed 3 days after isolation. Cell mixtures were grown in stimulation medium lacking PHA (infection medium). Cells (3×10^5) were seeded in 100 μl infection medium in 96-well V-bottom plates and infected with equal amounts of the respective virus preparations (0.1 ng p24). Starting at 24 h p.i., samples of supernatant (95 μl) were removed at the indicated time points and replaced by fresh prewarmed infection medium. The amounts of p24 in the supernatant samples were quantified by ELISA.

Release assay and Vpr incorporation. Tissue culture supernatants from 293T cells transfected with the respective proviral plasmids were harvested at 30 h p.t. and cleared by filtration through a 0.45-μm filter, and particles were collected by ultracentrifugation through a 20% (wt/wt) sucrose cushion, sometimes followed by centrifugation through an Optiprep gradient (38). Cell lysates and particles were separated by SDS-polyacrylamide gel electrophoresis (PAGE) and transferred to a nitrocellulose membrane. Gag- and Vpr-derived proteins were detected by quantitative immunoblotting (LiCor) using polyclonal sheep antiserum raised against recombinant HIV-1 CA and polyclonal rabbit antiserum raised against synthetic HIV-1 Vpr, as well as secondary antibodies and protocols provided by the manufacturer. Band intensities were quantified using the LiCor Odyssey 3.0 software, and relative release was quantitated by dividing total amounts of CA-reactive bands in the particle fraction by the total CA-reactive bands in cell lysates and particles.

Phosphopeptide mass spectrometry analysis. Virus particles were purified from the tissue culture medium of transfected 293T cells (NL4-3,

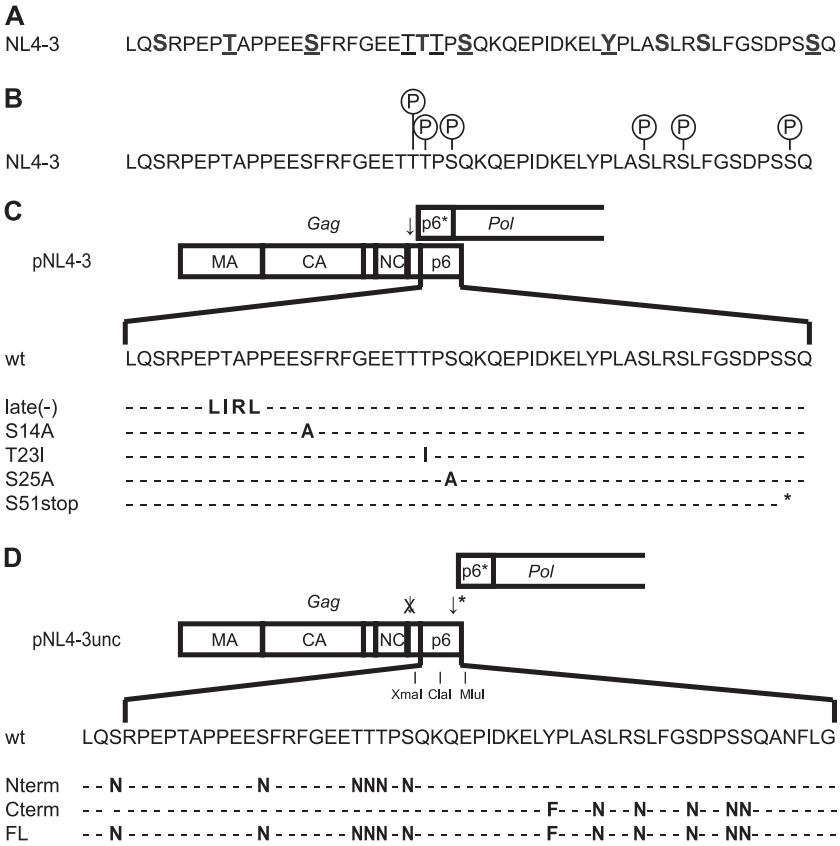

FIG 1 Schematic representation of potential p6 phosphorylation sites and p6 sequences of mutated viruses used in this study. (A) Amino acid sequence of HIV-1_{NL4-3} p6. Conserved residues among HIV-1 group M isolates (see Fig. S1 in the supplemental material) are shown in boldface. Residues that were predicted to be phosphorylated by the NetPhos algorithm (http://www.cbs.dtu.dk/services/NetPhos/) are underlined (see Table S1 in the supplemental material). (B) Phosphorylated residues within NL4-3 p6 isolated from viral particles. The circled P symbols indicate residues in p6 that we identified by mass spectrometry as phosphorylated in virion-associated Gag products (see Table S2 in the supplemental material). (C) Scheme of the *gag* and *pol* ORFs in the HIV-1_{NL4-3} genome. The arrow indicates the position of the Gag-Pol frameshift signal. Amino acid sequences of wt p6 and mutant derivatives used in this study are shown; mutated residues are indicated. (D) Scheme of the *gag* and *pol* ORFs in the HIV-$1_{NL4-3unc}$ genome. The arrow with an asterisk indicates the newly introduced frameshift signal at the 3′ end of *gag*; the arrow with the cross indicates the mutated authentic frameshift signal. Restriction sites for XmaI, ClaI, and MluI were introduced to facilitate exchange of p6-encoding fragments. Amino acid sequences of the altered p6 and sequences of the mutated NL4-3_{unc} variants are shown below the scheme; mutated residues are indicated.

NL4-3_{unc}, and mutants) or infected MT-4 T cells (NL4-3) by centrifugation through a 20% (wt/wt) sucrose cushion, followed by ultracentrifugation through an OptiPrep gradient as described previously (38). Throughout the purification procedure, samples were supplemented with a phosphatase inhibitor cocktail (Phosphatase Inhibitor Cocktail Set V; Calbiochem). For phosphopeptide analysis of NL4-3-derived proteins, the purity of virus preparations was analyzed by SDS-PAGE, followed by silver staining. Virus concentrations were determined by p24 ELISA. Samples corresponding to 4 μg p24 were separated by SDS-PAGE (NuPAGE Bis-Tris 4 to 12% gel; Invitrogen). The positions of p6-containing bands were identified by parallel immunoblotting with a polyclonal antiserum raised against HIV-1 p6. The corresponding bands were excised from the gel and in-gel digested as described previously (39). For NL4-3_{unc} wt and mutant virus samples, particles were produced from 293T cells transfected with the respective proviral plasmids and grown in the presence of the HIV-1 protease inhibitor lopinavir (2 μM). Purified particles were resuspended in 0.9% NaCl solution supplemented with Halt Phosphatase Inhibitor Cocktail (Thermo Scientific) according to the manufacturer's instructions. Virus concentrations and purity were analyzed by SDS-PAGE, followed by silver staining. Samples corresponding to 2 μg Gag were separated by SDS-PAGE (NuPAGE Bis-Tris 4 to 12% gel; Invitrogen) and processed as described above.

Peptides were extracted with 50 μl 0.1% trifluoroacetic acid and 50 μl 0.1% trifluoroacetic acid-acetonitrile (50:50) for 15 min each, and the two extracts were combined. NL4-3-derived phosphopeptides were enriched using titanium dioxide (TiO_2) (40). Sample preparation was conducted as described previously (41). Samples were analyzed by nano-liquid chromatography tandem mass spectrometry (LC–MS-MS) on an LTQ Orbitrap Velos (Thermo Scientific) mass spectrometer coupled to an Ultimate 3000 nano-high-performance liquid chromatograph (HPLC) (Thermo Scientific). Peptides were preconcentrated on a self-packed Synergi HydroRP trapping column (100-μm inner diameter; 4-μm particle size; 100-Å pore size; 2-cm length) and separated on a self-packed Synergi HydroRP main column (75-μm inner diameter; 2.5-μm particle size; 100-Å pore size; 30-cm length) at 60°C and a flow rate of 270 nl/min using a binary gradient (A, 0.1% formic acid; B, 0.1% formic acid, 84% acetonitrile) ranging from 5% to 50% B in 50 min. MS survey scans were acquired from 350 to 2,000 *m/z* in the Orbitrap at a resolution of 60,000 using the polysiloxane *m/z* 445.120030 as lock mass (42). The five most intense signals were subjected to collision-induced dissociation (CID)-based MS-MS in the LTQ using a normalized collision energy of 35%, an activation time of 30 ms, and a dynamic exclusion of 10 s. Automatic gain control (AGC) values were set to 10^6 for MS and 10^4 for MS-MS scans.

Raw data were processed using the Proteome Discoverer software V1.3

(Thermo Scientific) and searched against a Swiss-Prot virus database (14,986 target sequences; 8 February 2011) using Mascot (version 2.3.2) and Sequest with the following settings: 10-ppm MS tolerance, 0.4-Da MS-MS tolerance, trypsin as the enzyme allowing a maximum of 2 missed cleavage sites, and carbamidomethylation of cysteine as fixed modifications and oxidation of methionine, as well as phosphorylation of S/T/Y, as variable modifications. Peptide Validator and phosphoRS (43) nodes were used to assess global false-discovery rates and phosphorylation site localization probabilities, respectively. The results were filtered for mass deviations of ≤4 ppm and high confidence (corresponding to a false-discovery rate of <1% with Peptide Validator).

Microscopy and single-virus tracking. HeLa cells were seeded at 1.5×10^4 cells/well into 8-well glass bottom chamber slides (LabTek; Nunc). After 24 h of incubation at 37°C, the cells were transfected with equimolar amounts (500 ng DNA/well) of either $pCHIV_{unc}$ and $pCHIV_{unc}^{eGFP}$, or $pCHIV_{unc}$ FL and $pCHIV_{unc}^{eGFP}$ FL, respectively, using Fugene 6 (Roche) according to the manufacturer's instructions. At 20 h p.t., the cells were transferred into imaging buffer (25 mM Na-HEPES [pH 7.4], 137 mM NaCl, 2.7 mM KCl, 1 mM $CaCl_2$, and 30 mM glucose), and live-cell total internal reflection fluorescence microscopy (TIR-FM) was performed.

The TIR-FM setup (Visitron) used here is based on a Zeiss Axiovert 200 M fluorescence microscope equipped with an alpha plan Fluar 100×/1.45 oil immersion objective and an electron-multiplying charge-coupled-device (EM-CCD) camera (Cascade II; Roper Scientific; 512 by 512 pixels). The details of the setup have been described previously (35). Image acquisition was performed using Metamorph V6.3r7. Image analysis, identification of individual assembly sites, and single-virus tracing were performed using an automated particle-tracking algorithm as described previously (44, 45). Changes in Gag^{eGFP} fluorescence intensity at individual HIV-1 assembly sites were analyzed over time, and exponential assembly phases from multiple individual sites were aligned and averaged as described previously (45). The data were fitted to a saturating exponential function using GraphPad Prism 5 to determine average rate constants of HIV-1 assembly.

RESULTS

Prediction of potentially phosphorylated amino acids in HIV-1 p6. To test whether phosphorylation of p6 is functionally relevant for HIV-1 replication, we initially wanted to analyze the consequences of mutating individual phosphorylatable residues within p6 for viral replication. Phosphoamino acid analysis had revealed that p6 is phosphorylated at multiple sites and that serine, threonine, and tyrosine residues can be phosphorylated (18). Since 13 of the 52 amino acids of $HIV\text{-}1_{NL4\text{-}3}$ p6 are potentially phosphorylatable (Fig. 1A), we first selected appropriate candidate residues for individual mutational analysis. Reasoning that functionally relevant candidates should be (i) highly conserved, (ii) recognized by cellular kinases, and (iii) detectably phosphorylated in HIV-1 p6, we first checked for conservation among different subtypes of HIV-1 type M based on Gag sequence data obtained from the Los Alamos database (http://www.hiv.lanl.gov/). As shown in Fig. 1A and Fig. S1 in the supplemental material, most phosphorylatable residues in the p6 region are highly conserved among the subtype consensus sequences. Second, we performed a search using the NetPhos phosphorylation site prediction program (http://www.cbs.dtu.dk/services/NetPhos/) to identify residues predicted to be phosphorylated by known kinases based on their primary sequence context (46). Figure 1A summarizes the residues considered most likely to be phosphorylated based on the ranking by the NetPhos algorithm (see Table S1 in the supplemental material). This comprises residues T8, S14, T21, T23, S25, Y36, and S51. Finally, we isolated p6-containing proteins from highly purified HIV-1 particles to directly determine which residues were actually phosphorylated. Tryptic fragments were analyzed by LC–MS-MS following enrichment of phosphopeptides by titanium dioxide affinity chromatography (see Table S2 in the supplemental material). Residues T22/23, S25, S40, S43, and S51 were repeatedly detected as being phosphorylated in p6 or intermediate p6 processing products in virus preparations from transfected 293T or infected MT-4 cells (Fig. 1B; see Table S2 in the supplemental material). Only a subset of these residues was found to be phosphorylated in each individual sample, however (see Table S2 in the supplemental material). Whether the different patterns observed reflect cell-type-specific differences, dynamic changes, or simply subtle technical differences in sample preparation and analysis remains to be determined.

Effects of mutation of individual p6 residues. Based on the data summarized in Fig. 1A and B (see Figure S1 and Tables S1 and S2 in the supplemental material), we selected residues S14, T23, S25, and S51 for mutagenesis. Residue S40 was omitted because a detailed analysis of an HIV-1 p6 mutant, S40F, had recently been performed (26). Residue T8 was not included because it is part of the essential PTAP motif (11), and residue S43 was not included because an S43A mutation had no apparent effect on HIV-1 release (16). The respective constructs are summarized in Fig. 1C; S14 and S25 were changed to alanine, T23 to isoleucine, and S51 to a stop codon. The last two mutations retained the amino acid sequence in the overlapping *pol* reading frame, while the S14A and S25A changes led to alterations from glutamate to glycine and from leucine to arginine in residues 30 and 41 of Pol, respectively. An HIV-1 variant in which the PTAP sequence was mutated to LIRL ["late(−)"] in order to block recruitment of ESCRT-I (47) was included as a control for impaired p6 function in HIV-1 particle release (Fig. 1C).

293T cells were transfected with pNL4-3 or the mutated proviral plasmids. Cell lysates and particles were harvested 30 h p.t. and analyzed by quantitative immunoblotting using antiserum against HIV-1 CA (Fig. 2A). The wt samples showed the expected processing pattern, with mainly Gag and intermediate processing products detected in the cell lysates and predominantly mature CA in the particle fractions. The late(−) control virus displayed reduced release efficiency. It also showed the increased amount of the intermediate CA processing product CA-SP1 typically observed upon impairment of p6 function (47). In contrast, mutations at individual phosphorylatable residues in p6 did not result in detectable alterations of Gag processing or particle release compared to the wt. This visual impression was confirmed by quantitative analysis of four individual experiments. With the exception of the late(−) control, the relative release efficiencies of the variants did not significantly differ from that of wt virus (Fig. 2B). The single-round infectivity of the released particles (normalized for particulate antigen) was tested by titration on HeLa TZM-bl indicator cells, which express luciferase driven by an HIV-1 Tat-dependent long terminal repeat (LTR) promoter. As shown in Fig. 2C, none of the p6 variants except the late(−) control showed a significant decrease in relative infectivity compared to NL4-3 wt. The late(−) virus was strongly reduced in relative infectivity, in agreement with the observed impairment of proteolytic Gag maturation.

Comprehensive mutational analysis of p6 phosphorylation sites. The results described so far demonstrate that phosphorylation of p6 at individual residue S14, S25, T23, or S51 is not required for HIV-1 particle release or infectivity. Conceivably, phos-

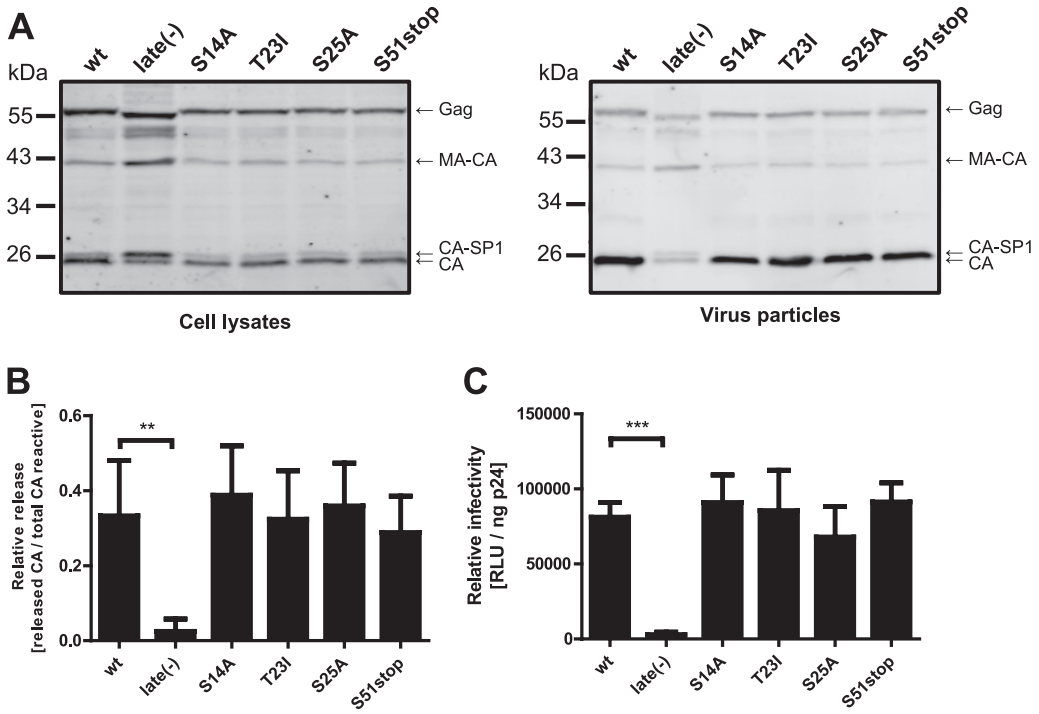

FIG 2 Effects of single mutations in p6 on Gag processing, viral release, and infectivity. (A) Gag processing and particle release efficiency. Virus particles were prepared by ultracentrifugation from the tissue culture supernatant of 293T cells transfected with the indicated proviral plasmids. Cell lysates (left) and virus particles (right) were analyzed for Gag-derived products by quantitative immunoblotting (LiCor) using antiserum raised against recombinant HIV-1 CA. The positions of molecular mass standards are shown on the left, and Gag-derived proteins are indicated on the right. (B) Quantitative immunoblotting of cell lysates and particles shown in panel A was used to calculate the amount of CA released, normalized to total anti-CA reactive proteins as described in Materials and Methods. Mean values and standard deviations (SD) from four independent experiments are shown. (C) Single-round virus infectivity. 293T cells were transfected with the indicated pNL4-3 derivatives. Supernatants were harvested at 30 h p.t., and infectivity was quantitated by titration on TZM-bl reporter cells, as described in Materials and Methods. Values were normalized for virus amounts as determined by p24 ELISA. The mean values and SD from four independent experiments are shown. *P* values in panels B and C were calculated using an unpaired Student's *t* test (**, $P < 0.01$; ***, $P < 0.001$). Comparison of S14A, T23I, S25A, and S51stop to the wt yielded nonsignificant *P* values.

phorylation at residues not included in our analysis may still be crucial, however. In addition, redundant phosphorylation may occur at one or several possible acceptor sites, which cannot be determined by mutagenesis of individual sites. We therefore embarked on a comprehensive mutational analysis of all phosphorylatable residues in HIV-1 p6. Mutations in *p6* also affect the sequence of the overlapping *p6* pol* region and may, in addition, influence frameshifting efficiency, thereby confounding the interpretation of results. To address this problem, we made use of a recently described HIV-1 derivative in which the *gag* and *pol* reading frames are uncoupled by mutagenesis of the authentic frameshift signal in conjunction with a short sequence duplication introducing a functional frameshift signal directly upstream of the *gag* stop codon (34). In this context, mutations within *p6* do not affect the primary sequence of Pol. Applying this strategy, we generated a *gag-pol* uncoupled variant of pNL4-3 (pNL4-3_{unc}) (Fig. 1D). Silent unique restriction sites were introduced to facilitate the exchange of p6-encoding fragments.

Virus release and Gag proteolytic maturation of HIV-$1_{NL4\text{-}3unc}$ were compared to those of wt HIV-1 by transfecting 293T cells with pNL4-3_{unc} and pNL4-3, followed by quantitative immunoblot analysis of cell lysates and viral particles. A slightly lower electrophoretic mobility of Gag indicated the presence of five additional amino acids at the C terminus of Gag of NL4-3_{unc}, while Gag processing was not impaired by the introduced mutations (Fig. 3A). Quantitative evaluation of immunoblot data confirmed that there was no significant difference in relative virus release between NL4-3 and NL4-3_{unc} (Fig. 3B). Viral infectivity was tested by single-round infection of TZM-bl indicator cells (Fig. 3C) and by endpoint titration on C8166 T cells (Fig. 3D). In accordance with previous results (34), we observed a tendency toward slightly reduced infectivity of NL4-3_{unc} in both assays, but the observed reduction was not statistically significant.

We subsequently constructed a derivative of pNL4-3_{unc} carrying mutations in all possible phosphorylation sites in p6, with the exception of T8, which is part of the essential PTAP late-domain motif (termed pNL4-3_{unc} FL) (Fig. 1D). The remaining 11 serine and threonine residues were changed to asparagine, and the single tyrosine residue was changed to phenylalanine. These conservative exchanges were chosen to retain the chemical properties of the original residues as much as possible. Besides an exchange of phosphorylatable residues in the entire p6 domain, two additional constructs were made, in which either six N-terminal or six C-terminal phosphorylatable residues were exchanged (pNL4-3_{unc} Nterm and pNL4-3_{unc} Cterm, respectively) (Fig. 1D). The respective proviral plasmids were transfected into 293T cells, and cell lysates and viral particles were collected and analyzed. Phosphorylation of Gag proteins was determined by LC–MS-MS analysis of Gag isolated from highly purified immature HIV-$1_{NL4\text{-}3unc}$ (wt, Nterm, Cterm, and FL). These analyses revealed no obvious

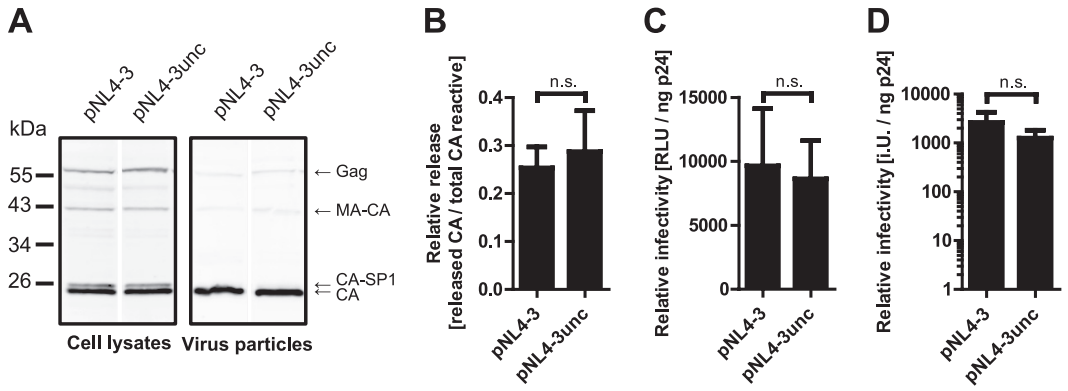

FIG 3 Effect of uncoupling the HIV-1 *gag* and *pol* reading frames on Gag processing, viral release, and infectivity. (A) Gag processing and release. 293T cells were transfected with the indicated proviral plasmids. At 30 h p.t., cell lysates (left) and tissue culture supernatants (right) were harvested, and virus particles were prepared by ultracentrifugation from the supernatant. Samples were separated by SDS-PAGE, and Gag-derived proteins were detected by quantitative immunoblotting (LiCor) using polyclonal antiserum raised against recombinant HIV-1 CA. The positions of molecular mass standards are shown on the left, and Gag-derived proteins are indicated on the right. (B) Results from the quantitative immunoblot analysis shown in panel A were used to calculate relative release efficiencies, as described in Materials and Methods. Mean values and SD from five independent experiments are shown. (C and D) Relative infectivities of tissue culture supernatants harvested from 293T cells transfected with the indicated proviral plasmids. (C) Single-round infectivity was determined by titration of virus on TZM-bl cells, as for Fig. 2C. (D) Infectivity on C8166 T cells was determined by endpoint titration, as described in Materials and Methods. The values were normalized for the amount of virus, as determined by p24 ELISA. The graphs show means and SD of at least three independent experiments. (B to D) Nonsignificance (n.s.) was determined by an unpaired Student's *t* test.

change in the phosphorylation status of the MA and CA domains upon mutation of phosphorylatable residues within p6. Phosphorylation in the p6 domain itself was completely lost in the case of the FL mutant, however. Consistent with the respective mutations, the Nterm mutant virus retained only phosphorylation of p6 residue S40 (close to the C terminus of p6), and the Cterm variant retained phosphorylation at T22/23 and S25 (in the N-terminal part of p6). No new phosphorylation sites within p6 were detected in any of the variant Gag proteins, suggesting that removal of phosphorylatable residues did not result in compensatory phosphorylation at other sites.

Inspection of Gag processing patterns on immunoblots of cell lysates and particles (Fig. 4A) showed no detectable processing impairment for any of the variants in the particle fraction. A subtle increase in the relative amount of CA-SP1 was observed in cells expressing the Cterm and FL variants, while processing was completely unaffected for the Nterm variant (Fig. 4A). Particle release was unaffected for all three variants compared to the wt (Fig. 4B). Since the p6 domain mediates incorporation of the viral protein R (Vpr) into the virion (48), we examined whether the extensive mutations affected Vpr particle incorporation. As shown in Fig. 4C, Vpr incorporation was retained in all three variants. Comparison of relative Vpr incorporation (Fig. 4D) revealed an ~2-fold reduction of Vpr in the Nterm and FL viruses compared to the wt. No difference in Vpr incorporation was observed between the wt and the Cterm variant despite mutation of three serine residues (at positions 40, 43, and 47) that flank, or are part of, the LRSLFG Vpr incorporation motif (16) in p6. These results suggest that other regions of p6 outside the known incorporation motif may also affect Vpr uptake by HIV-1.

To assess potential differences in viral assembly kinetics, live-cell microscopy was performed for wt and FL virus. These experiments made use of a previously established system where Gag is labeled by insertion of EGFP between the MA and CA domains of the protein (resulting in plasmid pCHIV^{eGFP} [35]). This construct leads to the formation of fluorescently labeled viral particles with wt efficiency and wt particle morphology if cotransfected together with an equimolar amount of its unlabeled counterpart. Assembly of individual virus particles can then be directly observed by live-cell TIR-FM at the membranes of virus-expressing cells (45). The *gag-pol* regions of pNL4-3$_{unc}$ and pNL4-3$_{unc}$ FL were transferred into the context of pCHIV^{eGFP}, and Gag assembly kinetics were investigated in HeLa cells transfected with the respective constructs (Fig. 5; see Movies S1 and S2 in the supplemental material). As previously observed for HIV^{eGFP}, cells expressing HIV$_{unc}^{eGFP}$ or HIV$_{unc}^{eGFP}$ FL displayed a gradual accumulation of punctate assembly sites at the plasma membrane over a period of 1 to 2 h (Fig. 5A and Movies S1 and S2). Detailed analysis of assembly kinetics over the exponential phase of Gag accumulation (Fig. 5B) yielded average rate constants of 0.0057 ± 0.0035 s^{-1} for HIV$_{unc}^{eGFP}$ and 0.0045 ± 0.0025 s^{-1} for HIV$_{unc}^{eGFP}$ FL, respectively. These rates are similar to the rate constant of 0.0043 ± 0.00054 s^{-1} previously determined for HIV^{eGFP} (45). There was no significant difference between the constructs carrying wt p6 or its FL variant, indicating that alteration of all but one phosphorylatable residue in p6 did not alter HIV-1 Gag assembly rates. Of note, a variant with a mutation of T8 in the context of a PTAP late-domain change to LIRL had been analyzed in a previous study, which showed no alteration of Gag assembly rates (45).

We proceeded to test the infectivity of the variants on TZM-bl (Fig. 6A) and C8166 (Fig. 6B) cells. There was no reduction in infectivity for NL4-3$_{unc}$ Nterm compared to wt NL4-3$_{unc}$ in either of these cell lines. A slight reduction was observed for NL4-3$_{unc}$ FL and NL4-3$_{unc}$ Cterm compared to wt NL4-3$_{unc}$ in single-round infectivity on TZM-bl cells. Subtle decreases in the infectious titers of these variants on C8166 cells were not statistically significant, however (Fig. 6A and B). Finally, the effect of the *p6* alterations on HIV-1 replication capacity was assessed in primary T cells. Virus particles produced from transfected 293T cells were used to infect human PBMCs, and viral spread was monitored over a period of 13 days by quantitation of HIV-1 antigen released into the culture medium.

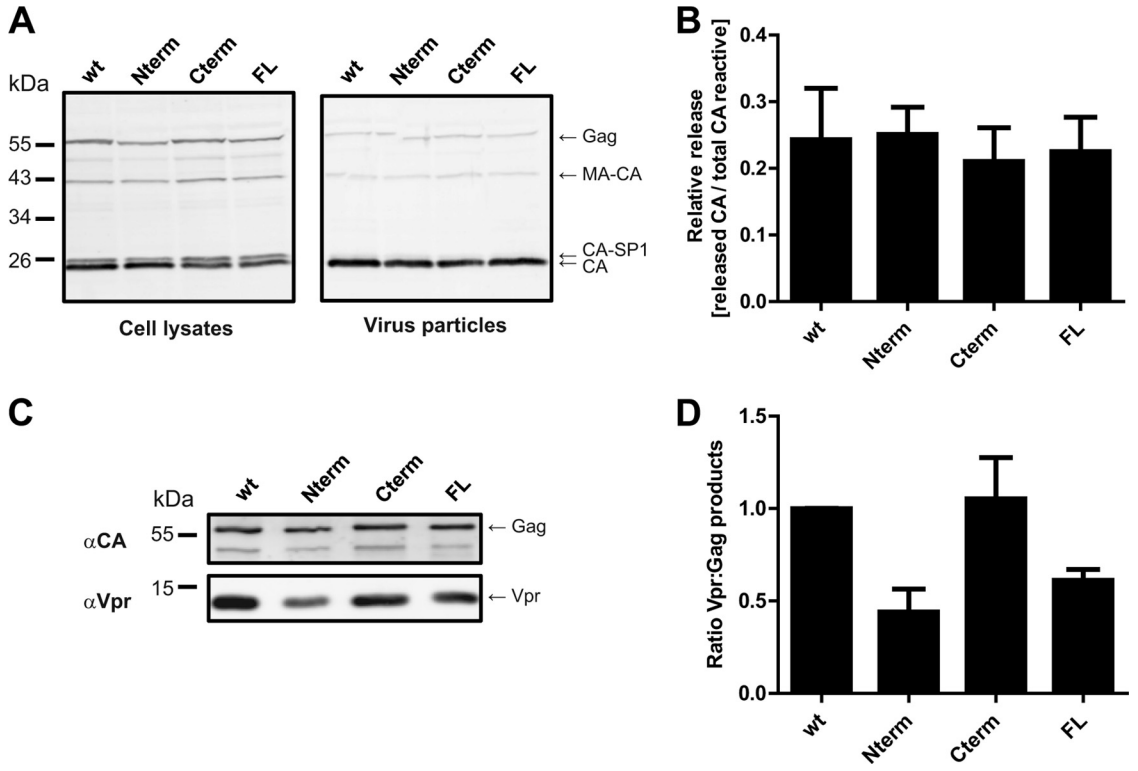

FIG 4 Effect of multiple mutations in p6 on Gag processing, viral release, and Vpr incorporation into viral particles. (A) Gag processing and release efficacy. Virions were purified from tissue culture supernatants of 293T cells transfected with the indicated proviral plasmids by ultracentrifugation through a sucrose cushion. Samples were separated by SDS-PAGE, and Gag-derived products from cell lysates (left) or virus pellets (right) were analyzed by quantitative immunoblotting (LiCor) using antiserum raised against recombinant HIV-1 CA. The positions of molecular mass standards are shown on the left, and Gag-derived proteins are indicated on the right. (B) Relative particle release efficiencies. Quantitative immunoblots shown in panel A were used to determine the amounts of CA released, normalized to total anti-CA reactive proteins expressed, as described in Materials and Methods. The graph shows mean values and SD from five independent experiments. (C) Vpr incorporation. Virions were purified from tissue culture supernatants of 293T cells transfected with the respective plasmids and cultured in the presence of 2 μM lopinavir by ultracentrifugation through an OptiPrep gradient. Samples were separated by SDS-PAGE, and viral particles were analyzed by quantitative immunoblotting (LiCor) using the indicated antisera. The positions of molecular mass standards are shown on the left, and proteins are indicated on the right. (D) Quantification of Vpr incorporation. The relative ratio of Vpr to Gag was calculated based on integrated band intensities from quantitative immunoblots, as shown in panel C. The graph shows mean values and SD from three independent experiments. The values were normalized to the ratio determined for the respective wt control.

Figure 6C shows the results of parallel infections of PBMCs from three blood donors (always used as mixtures of PBMCs from two donors) with three independent virus preparations of NL4-3_{unc} and the three p6 variants. NL4-3_{unc} FL, as well as the variants with alterations in either half of p6, replicated efficiently in PBMCs, reaching titers similar to those of the NL4-3_{unc} control at day 7 p.i. Small but significant reductions in titer compared to the NL4-3_{unc} control were observed for variants NL4-3_{unc} Cterm and NL4-3_{unc} FL at earlier time points (day 3 or 5) in cultures containing PBMCs from donor B, suggesting that these two variants may display a very subtle donor-dependent delay in replication in primary cells. To determine whether reversion of the introduced mutation(s) or recombination of the short duplicated sequence occurred upon prolonged passage, we analyzed the relevant region of the viral genomic RNA in tissue culture media from infected PBMCs. RNA was extracted from the culture medium collected from day 1 to day 13 p.i. and subjected to reverse transcriptase PCR. No recombination products were detected up to the peak of viral replication at day 7 p.i. (see Fig. S2 in the supplemental material). Sequencing of the predominant band from the sample taken at day 13 p.i. confirmed that all mutations introduced into the *p6* region were still present. We thus conclude that the growth properties determined in this study reflect the replication phenotype of the respective mutated virus.

DISCUSSION

Based on our previous observation that p6 is the major phosphopeptide of HIV-1 and that it can be phosphorylated at multiple sites (18), we have identified several residues that are phosphorylated in virion-associated p6 by mass spectrometry. Individual mutation of selected residues had no effect on virus assembly, release, and infectivity, suggesting that phosphorylation of any one of these residues may not be important. Phosphorylation sites are often redundant (27), however, and alteration of several potential phosphoacceptor sites may be required to reveal a potential phenotype. We therefore performed a comprehensive mutational analysis by altering all potentially phosphorylatable residues in p6. The only exception was residue T8, which was retained in all constructs as part of the functionally essential PTAP late-domain motif. Unexpectedly, changing 11 serine and threonine residues to asparagine and the single tyrosine residue to phenylalanine had no effect on virus release and only very minor effects on HIV-1 infectivity in two different cell lines and in primary cells. Passage of the

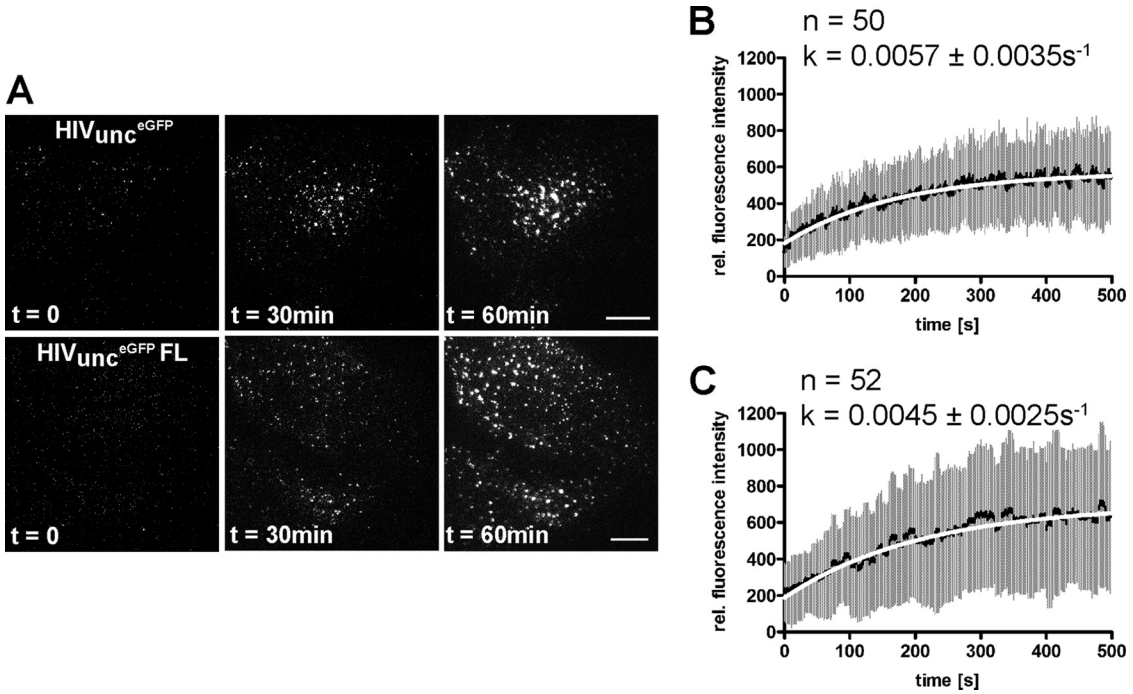

FIG 5 Effect of HIV-1 Gag p6 full-length phosphorylation mutation on HIV-1 assembly kinetics. HeLa cells were cotransfected with an equimolar ratio of either pCHIV$_{unc}$/pCHIV$_{unc}^{eGFP}$ (A, top row) or pCHIV$_{unc}$ FL/pCHIV$_{unc}^{eGFP}$ FL (A, bottom row). TIR-FM imaging was initiated at 12 h p.t. Cells expressing detectable amounts of Gag^{eGFP} that displayed only a low number of budding sites, detected as individual punctae at the plasma membrane, were selected for acquisition of image series with a time resolution of 2 s per frame. Shown are selected frames from Movies S1 (top) and S2 (bottom) in the supplemental material corresponding to the indicated time points. The scale bars represent 10 μm. (B and C) Average Gag assembly rates. Individual assembly sites from 50 and 52 different cells expressing HIV$_{unc}^{eGFP}$ (B) or HIV$_{unc}^{eGFP}$ FL (C), respectively, were tracked, and exponential assembly phases were averaged as described in Materials and Methods. The graphs show average intensities (black line) and SD (gray bars) from the indicated number (*n*) of individual sites. Assembly rate constants were determined by fitting the data to a saturating single exponential function (white line) using GraphPad Prism 5, yielding the indicated rate constants, *k*. rel., relative.

NL4-3$_{unc}$ FL virus in PBMCs for ~2 weeks did not lead to a reversion of any of the introduced p6 mutations. Phosphopeptide analysis of mutant viruses confirmed the loss of phosphorylation in the altered regions of p6 and yielded no evidence for compensatory phosphorylation at other sites within Gag. We thus conclude that the observed phosphorylation of HIV-1 p6 in infected cells and virions is dispensable for HIV-1 particle formation, maturation, and infectivity in tissue culture. We cannot formally exclude the functional importance of a potential phosphorylation of p6 residue T8, which was not mutated in this study. However, our mass spectrometry analyses of Gag phosphopeptides provided no evidence for phosphorylation at the site.

Previous reports have described a phenotype for changes of potential phosphorylation sites in HIV-1 p6, suggesting an important contribution of p6 phosphorylation to HIV-1 replication in tissue culture. This included residue T23, which was reported to be phosphorylated by virion-associated Erk-2 kinase (25); phosphorylation of T23 was confirmed by our mass spectroscopy analysis. Hemonnot et al. reported that a T23A alteration impaired virus release efficiency and Gag processing. Late viral budding structures arrested at the plasma membrane were observed by electron microscopy, reminiscent of the phenotype of known ESCRT recruitment-deficient HIV-1 variants. Furthermore, single-round virus infectivity was reported to be reduced (25). In contrast, we did not observe a comparable phenotype for an individual T23I mutation or for the change of all phosphorylatable residues in the p6 N-terminal moiety (including T23) to asparagine residues. No defect in virus assembly, release, Gag polyprotein processing, or infectivity was detected for either of these variants compared to wt HIV-1. The previously analyzed T23A variant may have different properties from the T23I and T23N variants analyzed here. Since none of the residues chosen to replace T23 could be phosphorylated, the potential differences are clearly not related to phosphorylation, however. Phosphorylation at T23 may thus reflect a bystander effect caused by recruitment of Erk-2 to the viral assembly site. Alternatively, phosphorylation of this and/or other p6 residues may be important under specific conditions not reflected in common tissue culture analyses (e.g., cell-to-cell transmission or infection of special cell types), and this will be the topic of future studies.

Votteler et al. (26) reported a processing and infectivity phenotype for an S40F variant of p6. This nonconservative mutation was chosen to avoid potentially confounding changes in the overlapping *pol* region. The authors observed that this mutation resulted in decreased infectivity of viral particles in single-round infection and decreased replication efficiency in tissue culture. This was accompanied by morphological aberrations of the variant particles. A defect in proteolytic maturation of CA correlated with impaired formation of the mature conical core. In the current study, we showed that S40 of p6 can indeed be phosphorylated. Based on the results presented here, we suggest, however, that the pronounced phenotype reported for the S40F variant may

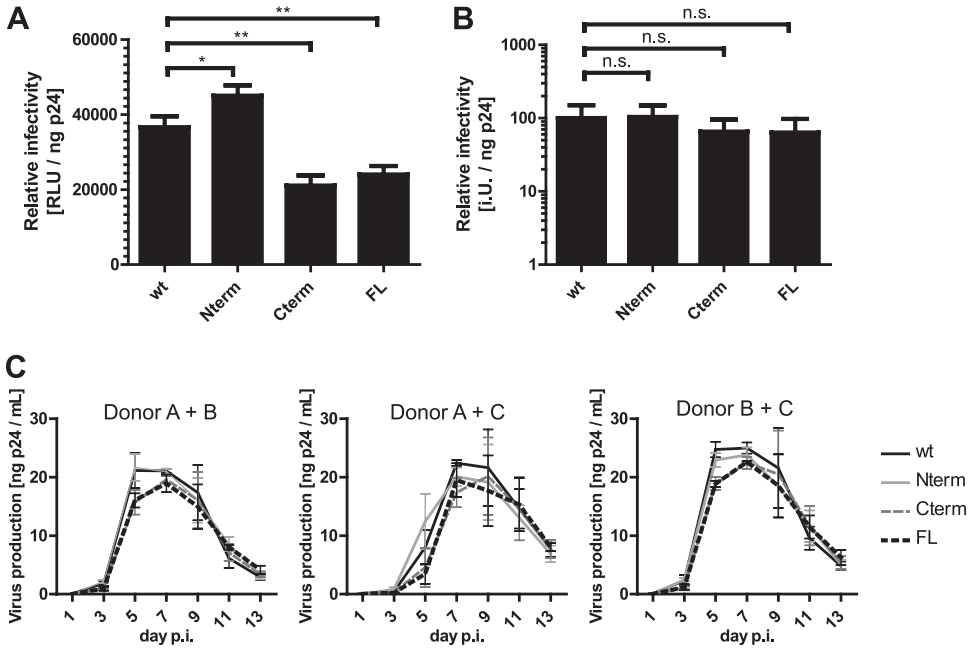

FIG 6 Effects of multiple mutations in p6 on viral infectivity and replication kinetics in primary cells. Viral particles were harvested from tissue culture supernatants of 293T cells transfected with plasmid pNL4-3$_{unc}$ or its indicated derivatives and were tested for replication competence in cell lines and primary T cells. (A and B) Relative infectivities in cell lines. (A) Single-round infectivity was assessed by titration of viral particles on TZM-bl cells as described in Materials and Methods. (B) Relative infectious titers on C8166 T cells were determined by endpoint titration as described in Materials and Methods. The values were normalized for virus amounts as determined by p24 ELISA. The graphs show means and SD of three independent experiments, normalized to the respective HIV-1$_{NL4-3unc}$ wt control. (A and B) *P* values were calculated using an unpaired Student's *t* test (n.s., $P > 0.05$; *, $P < 0.05$; **, $P < 0.01$). (C) Replication kinetics in primary cells. PBMCs were isolated using buffy coats from healthy blood donors and stimulated for 3 days using PHA and IL-2. Subsequently, samples from two individual donors each were mixed, and virus was added (0.1 ng p24/3 $\times$ 10^5 cells). Samples of tissue culture supernatants were collected at the indicated time points, and virus production was measured by p24 ELISA. The data shown are mean values and SD from three independent experiments using independent virus preparations. In each experiment, three different combinations of PBMCs (donors A plus B, B plus C, and A plus C) were tested.

be largely due to the very different chemical nature of the introduced phenylalanine residue. Exchange of all phosphorylatable residues in the C-terminal part of p6 (including S40) had only a minor effect on viral infectivity and CA processing. It is conceivable that the minor effects observed for the Cterm and FL constructs are due to the alteration of S40. Determining the relative contribution of any individual mutation would be difficult, however, given that the combination of six point mutations in this region displayed only a subtle effect on the viral phenotype.

The finding that mutating approximately one-fifth of all p6 residues did not affect virus assembly kinetics or release and had only a subtle effect on processing and infectivity was unexpected. Since several of these residues are highly conserved among all HIV-1 clades, we anticipated the FL variant would be noninfectious, requiring restoration of one or several essential residues to regain infectivity. However, sequence analysis of the HIV-1$_{unc}$ FL genome after 2 weeks of passage in tissue culture revealed no reversion of mutated residues. On the other hand, HIV-1 genomes undergo constant sequence alteration during viral replication *in vivo*, and tolerance of a large proportion of amino acid exchanges within an HIV-1 protein is not without precedent. Various studies have shown accumulation of a high number of mutations in HIV-1 occurring under selective drug pressure. For example, HIV-1 isolated from a patient under antiretroviral therapy was found to have acquired 19 nonsynonymous mutations in *PR* (corresponding to one-fifth of the PR primary sequence) without significantly lower viral titers (49). Conservation of p6 residues may also be caused, at least in part, by requirements imposed by the nearby frameshift signal and the overlapping *pol* reading frame. This makes it difficult to draw firm conclusions from the fact that a specific residue is conserved. The p6 domain appears to be largely unstructured, with only a weak helical propensity (14, 15). This feature is common for proteins that, like p6, serve as molecular adapters for several partners. Such flexibility may also increase mutational tolerance, as long as the overall hydrophilic profile is preserved. It is currently unclear whether p6 comprises any additional functional regions besides the small peptide motifs identified as binding Tsg101, ALIX, or Vpr. The experimental approach described here allows testing of this question by conservative mutagenesis of the entire p6 domain, except for its known functional modules. If a general high sequence flexibility of p6 could be confirmed, it would open the possibility of inserting linear peptide motifs with specific functional properties, thereby endowing lentiviral vectors with selected features.

ACKNOWLEDGMENTS

This work was supported in part by the Deutsche Forschungsgemeinschaft through the collaborative research grant SFB638 (project A9) and the Ministerium für Innovation, Wissenschaft und Forschung des Landes Nordrhein-Westfalen. H.-G.K. is an investigator of the excellence cluster CellNetworks (EXC81).

We thank Anke-Mareil Heuser and Maria Anders-Össwein for expert technical assistance.

REFERENCES

1. **Morikawa Y, Goto T, Sano K.** 1999. In vitro assembly of human immunodeficiency virus type 1 Gag protein. J. Biol. Chem. **274**:27997–28002.
2. **Gheysen D, Jacobs E, de Foresta F, Thiriart C, Francotte M, Thines D, De Wilde M.** 1989. Assembly and release of HIV-1 precursor Pr55gag virus-like particles from recombinant baculovirus-infected insect cells. Cell **59**:103–112.
3. **Briggs JA, Simon MN, Gross I, Krausslich HG, Fuller SD, Vogt VM, Johnson MC.** 2004. The stoichiometry of Gag protein in HIV-1. Nat. Struct. Mol. Biol. **11**:672–675.
4. **Carlson LA, Briggs JA, Glass B, Riches JD, Simon MN, Johnson MC, Muller B, Grunewald K, Krausslich HG.** 2008. Three-dimensional analysis of budding sites and released virus suggests a revised model for HIV-1 morphogenesis. Cell Host Microbe **4**:592–599.
5. **Fuller SD, Wilk T, Gowen BE, Krausslich HG, Vogt VM.** 1997. Cryo-electron microscopy reveals ordered domains in the immature HIV-1 particle. Curr. Biol. **7**:729–738.
6. **Sundquist WI, Krausslich HG.** 2012. HIV-1 assembly, budding, and maturation. Cold Spring Harb. Perspect. Med. **2**:a006924. doi:10.1101/cshperspect.a006924.
7. **Martin-Serrano J, Neil SJ.** 2011. Host factors involved in retroviral budding and release. Nat. Rev. Microbiol. **9**:519–531.
8. **Weiss ER, Gottlinger H.** 2011. The role of cellular factors in promoting HIV budding. J. Mol. Biol. **410**:525–533.
9. **Freed EO.** 2002. Viral late domains. J. Virol. **76**:4679–4687.
10. **von Schwedler UK, Stuchell M, Muller B, Ward DM, Chung HY, Morita E, Wang HE, Davis T, HE GP, Cimbora DM, Scott A, Krausslich HG, Kaplan J, Morham SG, Sundquist WI.** 2003. The protein network of HIV budding. Cell **114**:701–713.
11. **Gottlinger HG, Dorfman T, Sodroski JG, Haseltine WA.** 1991. Effect of mutations affecting the p6 gag protein on human immunodeficiency virus particle release. Proc. Natl. Acad. Sci. U. S. A. **88**:3195–3199.
12. **Baumgartel V, Ivanchenko S, Dupont A, Sergeev M, Wiseman PW, Krausslich HG, Brauchle C, Muller B, Lamb DC.** 2011. Live-cell visualization of dynamics of HIV budding site interactions with an ESCRT component. Nat. Cell Biol. **13**:469–474.
13. **Jouvenet N, Simon SM, Bieniasz PD.** 2011. Visualizing HIV-1 assembly. J. Mol. Biol. **410**:501–511.
14. **Fossen T, Wray V, Bruns K, Rachmat J, Henklein P, Tessmer U, Maczurek A, Klinger P, Schubert U.** 2005. Solution structure of the human immunodeficiency virus type 1 p6 protein. J. Biol. Chem. **280**:42515–42527.
15. **Stys D, Blaha I, Strop P.** 1993. Structural and functional studies in vitro on the p6 protein from the HIV-1 gag open reading frame. Biochim. Biophys. Acta **1182**:157–161.
16. **Kondo E, Gottlinger HG.** 1996. A conserved LXXLF sequence is the major determinant in p6gag required for the incorporation of human immunodeficiency virus type 1 Vpr. J. Virol. **70**:159–164.
17. **Ott DE, Coren LV, Copeland TD, Kane BP, Johnson DG, Sowder RC, II, Yoshinaka Y, Oroszlan S, Arthur LO, Henderson LE.** 1998. Ubiquitin is covalently attached to the p6Gag proteins of human immunodeficiency virus type 1 and simian immunodeficiency virus and to the p12Gag protein of Moloney murine leukemia virus. J. Virol. **72**:2962–2968.
18. **Muller B, Patschinsky T, Krausslich HG.** 2002. The late-domain-containing protein p6 is the predominant phosphoprotein of human immunodeficiency virus type 1 particles. J. Virol. **76**:1015–1024.
19. **Gao M, Karin M.** 2005. Regulating the regulators: control of protein ubiquitination and ubiquitin-like modifications by extracellular stimuli. Mol. Cell **19**:581–593.
20. **Guo Z, Kanjanapangka J, Liu N, Liu S, Liu C, Wu Z, Wang Y, Loh T, Kowolik C, Jamsen J, Zhou M, Truong K, Chen Y, Zheng L, Shen B.** 2012. Sequential posttranslational modifications program FEN1 degradation during cell-cycle progression. Mol. Cell **47**:444–456.
21. **Oskarsson MK, Long CW, Robey WG, Scherer MA, Vande Woude GF.** 1977. Phosphorylation and nucleic acid binding properties of m1 Moloney murine sarcoma virus-specific pP60gag. J. Virol. **23**:196–204.
22. **Yasuda J, Hunter E.** 1998. A proline-rich motif (PPPY) in the Gag polyprotein of Mason-Pfizer monkey virus plays a maturation-independent role in virion release. J. Virol. **72**:4095–4103.
23. **Kolesnikova L, Mittler E, Schudt G, Shams-Eldin H, Becker S.** 2012. Phosphorylation of Marburg virus matrix protein VP40 triggers assembly of nucleocapsids with the viral envelope at the plasma membrane. Cell. Microbiol. **14**:182–197.
24. **Clinton GM, Guerina NG, Guo HY, Huang AS.** 1982. Host-dependent phosphorylation and kinase activity associated with vesicular stomatitis virus. J. Biol. Chem. **257**:3313–3319.
25. **Hemonnot B, Cartier C, Gay B, Rebuffat S, Bardy M, Devaux C, Boyer V, Briant L.** 2004. The host cell MAP kinase ERK-2 regulates viral assembly and release by phosphorylating the p6gag protein of HIV-1. J. Biol. Chem. **279**:32426–32434.
26. **Votteler J, Neumann L, Hahn S, Hahn F, Rauch P, Schmidt K, Studtrucker N, Solbak SM, Fossen T, Henklein P, Ott DE, Holland G, Bannert N, Schubert U.** 2011. Highly conserved serine residue 40 in HIV-1 p6 regulates capsid processing and virus core assembly. Retrovirology **8**:11.
27. **Roach PJ.** 1991. Multisite and hierarchal protein phosphorylation. J. Biol. Chem. **266**:14139–14142.
28. **Wei X, Decker JM, Liu H, Zhang Z, Arani RB, Kilby JM, Saag MS, Wu X, Shaw GM, Kappes JC.** 2002. Emergence of resistant human immunodeficiency virus type 1 in patients receiving fusion inhibitor (T-20) monotherapy. Antimicrob. Agents Chemother. **46**:1896–1905.
29. **Scherer WF, Syverton JT, Gey GO.** 1953. Studies on the propagation in vitro of poliomyelitis viruses. IV. Viral multiplication in a stable strain of human malignant epithelial cells (strain HeLa) derived from an epidermoid carcinoma of the cervix. J. Exp. Med. **97**:695–710.
30. **Sena-Esteves M, Saeki Y, Camp SM, Chiocca EA, Breakefield XO.** 1999. Single-step conversion of cells to retrovirus vector producers with herpes simplex virus-Epstein-Barr virus hybrid amplicons. J. Virol. **73**:10426–10439.
31. **Salahuddin SZ, Markham PD, Wong-Staal F, Franchini G, Kalyanaraman VS, Gallo RC.** 1983. Restricted expression of human T-cell leukemia-lymphoma virus (HTLV) in transformed human umbilical cord blood lymphocytes. Virology **129**:51–64.
32. **Miyoshi I, Taguchi H, Fujishita M, Niiya K, Kitagawa T, Ohtsuki Y, Akagi T.** 1982. Asymptomatic type C virus carriers in the family of an adult T-cell leukemia patient. Gann **73**:339–340.
33. **Adachi A, Gendelman HE, Koenig S, Folks T, Willey R, Rabson A, Martin MA.** 1986. Production of acquired immunodeficiency syndrome-associated retrovirus in human and nonhuman cells transfected with an infectious molecular clone. J. Virol. **59**:284–291.
34. **Leiherer A, Ludwig C, Wagner R.** 2009. Uncoupling human immunodeficiency virus type 1 Gag and Pol reading frames: role of the transframe protein p6* in viral replication. J. Virol. **83**:7210–7220.
35. **Lampe M, Briggs JA, Endress T, Glass B, Riegelsberger S, Krausslich HG, Lamb DC, Brauchle C, Muller B.** 2007. Double-labelled HIV-1 particles for study of virus-cell interaction. Virology **360**:92–104.
36. **Wiegers K, Rutter G, Kottler H, Tessmer U, Hohenberg H, Krausslich HG.** 1998. Sequential steps in human immunodeficiency virus particle maturation revealed by alterations of individual Gag polyprotein cleavage sites. J. Virol. **72**:2846–2854.
37. **Reed LJ, Muench H.** 1938. A simple method of estimating fifty per cent endpoints. Am. J. Epidemiol. **27**:493–497.
38. **Dettenhofer M, Yu XF.** 1999. Highly purified human immunodeficiency virus type 1 reveals a virtual absence of Vif in virions. J. Virol. **73**:1460–1467.
39. **Zahedi RP, Sickmann A, Boehm AM, Winkler C, Zufall N, Schonfisch B, Guiard B, Pfanner N, Meisinger C.** 2006. Proteomic analysis of the yeast mitochondrial outer membrane reveals accumulation of a subclass of preproteins. Mol. Biol. Cell **17**:1436–1450.
40. **Larsen MR, Thingholm TE, Jensen ON, Roepstorff P, Jorgensen TJ.** 2005. Highly selective enrichment of phosphorylated peptides from peptide mixtures using titanium dioxide microcolumns. Mol. Cell. Proteomics **4**:873–886.
41. **Beck F, Lewandrowski U, Wiltfang M, Feldmann I, Geiger J, Sickmann A, Zahedi RP.** 2011. The good, the bad, the ugly: validating the mass spectrometric analysis of modified peptides. Proteomics **11**:1099–1109.
42. **Olsen JV, de Godoy LM, Li G, Macek B, Mortensen P, Pesch R, Makarov A, Lange O, Horning S, Mann M.** 2005. Parts per million mass accuracy on an Orbitrap mass spectrometer via lock mass injection into a C-trap. Mol. Cell. Proteomics **4**:2010–2021.
43. **Taus T, Kocher T, Pichler P, Paschke C, Schmidt A, Henrich C, Mechtler K.** 2011. Universal and confident phosphorylation site localization using phosphoRS. J. Proteome Res. **10**:5354–5362.
44. **Godinez WJ, Lampe M, Worz S, Muller B, Eils R, Rohr K.** 2009. Deterministic and probabilistic approaches for tracking virus particles in time-lapse fluorescence microscopy image sequences. Med. Image Anal. **13**:325–342.

45. **Ivanchenko S, Godinez WJ, Lampe M, Krausslich HG, Eils R, Rohr K, Brauchle C, Muller B, Lamb DC.** 2009. Dynamics of HIV-1 assembly and release. PLoS Pathog. **5**:e1000652. doi:10.1371/journal.ppat.1000652.
46. **Blom N, Gammeltoft S, Brunak S.** 1999. Sequence and structure-based prediction of eukaryotic protein phosphorylation sites. J. Mol. Biol. **294**: 1351–1362.
47. **Huang M, Orenstein JM, Martin MA, Freed EO.** 1995. p6Gag is required for particle production from full-length human immunodeficiency virus type 1 molecular clones expressing protease. J. Virol. **69**:6810–6818.
48. **Kondo E, Mammano F, Cohen EA, Gottlinger HG.** 1995. The p6gag domain of human immunodeficiency virus type 1 is sufficient for the incorporation of Vpr into heterologous viral particles. J. Virol. **69**:2759–2764.
49. **Kozisek M, Henke S, Saskova KG, Jacobs GB, Schuch A, Buchholz B, Muller V, Krausslich HG, Rezacova P, Konvalinka J, Bodem J.** 2012. Mutations in HIV-1 gag and pol compensate for the loss of viral fitness caused by a highly mutated protease. Antimicrob. Agents Chemother. **56**:4320–4330.